

21. M. A. Cane (*J. Phys. Oceanogr.*, in press) questions the adequacy of the linear theory.
22. The ocean circulation can be represented as the sum of an external (barotropic) mode, in which the entire vertical column responds as a unit, and an infinite number of internal (baroclinic) modes. Only the baroclinic response is important at the long time scales characteristic of El Niño.
23. R. A. Knox and D. Halpern, *J. Mar. Res.* **40** (Suppl.), 329 (1982); C. C. Eriksen *et al.*, *J. Phys. Oceanogr.*, in press.
24. D. Enfield, *J. Geophys. Res.* **86**, 2005 (1981).
25. Wind fields are composites from E. M. Rasmusson and T. H. Carpenter (15).
26. C. Ramage and A. M. Hori, *Mon. Weather Rev.* **110**, 587 (1982).
27. A. Leetmaa, *J. Phys. Oceanogr.* **13**, 467 (1983).
28. The currents slow in response to a weakening of the southeast trade winds.
29. P. Schopf, *J. Phys. Oceanogr.*, in press.
30. J. Sadler and B. Kilonsky, *Trop. Ocean-Atmos. Newsl.* **16**, 3 (1983).
31. G. Meyers and J. R. Donguy, *ibid.*, p. 8.
32. Available climatologies differ by more than 1°C in this area due to different averaging periods, data bases, and analysis techniques.
33. K. Wyrtki, *Trop. Ocean-Atmos. Newsl.* **16**, 6 (1983).
34. G. Meyers, private communication.
35. E. Firing, R. Lukas, J. Sadler, K. Wyrtki, *Science* **222**, 1121 (1983).
36. The Equatorial Undercurrent is a permanent (with the exception noted) feature in the Atlantic and Pacific. It is a subsurface, eastward-moving current at the equator with speeds often in excess of 1 m/sec.
37. In May 1983 a westward jet was also found at normal undercurrent depth at 95°W (S. Hayes, private communication).
38. R. L. Smith, *Science* **221**, 1397 (1983).
39. *Spec. Clim. Diagn. Bull.* (15 July 1983) (available from Climate Analysis Center, NOAA, Washington, D.C. 20233).
40. The significance of these excursions was first noted by K. Wyrtki [*Mar. Technol. Soc. J.* **16**, 3 (1982)].
41. Courtesy of R. Reynolds.
42. Island station data are courtesy of K. Wyrtki; Callao data are from D. Enfield and S. P. Hayes [*Trop. Ocean-Atmos. Newsl.* **21**, 13 (1983)].
43. A. Leetmaa, D. Behringer, J. Toole, R. Smith, *ibid.*, p. 11.
44. I thank the many colleagues who reviewed an early version of the manuscript. Special thanks are extended to those who generously contributed unpublished data and to Lenny Martin for assistance in preparing the manuscript. This work was supported by grant OCE-8214771 from the National Science Foundation.

Meteorological Aspects of the El Niño/Southern Oscillation

Eugene M. Rasmusson and John M. Wallace

Each year various parts of the globe experience regional climate anomalies such as droughts, record cold winters, and unusual numbers of storms. But some years, such as 1982 and 1983, are

and named by Sir Gilbert Walker more than a half-century ago (1). The primary manifestation of the Southern Oscillation is a seesaw in atmospheric pressure at sea level between the southeast Pacific

Summary. The single most prominent signal in year-to-year climate variability is the Southern Oscillation, which is associated with fluctuations in atmospheric pressure at sea level in the tropics, monsoon rainfall, and wintertime circulation over North America and other parts of the extratropics. Although meteorologists have known about the Southern Oscillation for more than a half-century, its relation to the oceanic El Niño phenomenon was not recognized until the late 1960's, and a theoretical understanding of these relations has begun to emerge only during the past few years. The past 18 months have been characterized by what is probably the most pronounced and certainly the best-documented El Niño/Southern Oscillation episode of the past century. In this review meteorological aspects of the time history of the 1982–1983 episode are described and compared with a composite based on six previous events between 1950 and 1975, and the impact of these new observations on theoretical interpretations of the event is discussed.

characterized by large, remarkably coherent climate anomalies over much of the globe. The pattern inherent in these anomalies has been recognized gradually, over a period of decades, as a result of the collection and analysis of many different climatic records; the recognition process has been somewhat like the assembly of a global-scale jigsaw puzzle.

Some of the pieces of this puzzle are implicit in the Southern Oscillation, a coherent pattern of pressure, temperature, and rainfall fluctuations discovered

subtropical high and the region of low pressure stretching across the Indian Ocean from Africa to northern Australia. Other manifestations involve surface temperatures throughout the tropics and monsoon rainfall in southern Africa, India, Indonesia, and northern Australia (2, 3). When Walker's scientific contemporaries expressed doubts concerning these statistical relations because of the lack of a physically plausible mechanism for linking climate anomalies in far-flung regions of the globe, he replied, "I think

the relationships of world weather are so complex that our only chance of explaining them is to accumulate the facts empirically . . . there is a strong presumption that when we have data of the pressure and temperature at 10 and 20 km, we shall find a number of new relations that are of vital importance" (4).

Descriptive studies of the 1957–1958 El Niño event, based in part on routine merchant ship data from the tropical Pacific, were instrumental in revealing the link between El Niño and the Southern Oscillation. The large-scale interaction between atmosphere and ocean was confirmed by retrospective statistical studies of past episodes (5). The emerging unified view of the El Niño/Southern Oscillation (ENSO) phenomenon is exemplified by Bjerknes's investigations (6) of the 1957–1958, 1963–1964, and 1965–1966 ENSO episodes. These studies were among the first in which satellite imagery was used to define the region of anomalously heavy rainfall over the dry zone of the equatorial central and eastern Pacific during episodes of warm sea-surface temperature (SST), an aspect of the phenomenon that Walker apparently was unaware of. Bjerknes showed that these fluctuations in SST and rainfall are associated with large-scale variations in the equatorial trade wind systems, which in turn reflect the major variations of the Southern Oscillation pressure pattern.

The linking of El Niño with the Southern Oscillation was viewed as evidence that ocean circulation plays the role of a flywheel in the climate system and is responsible for the extraordinary persistence of the atmospheric anomalies from month to month and sometimes even

Eugene M. Rasmusson is chief, Diagnostics Branch, Climate Analysis Center, National Meteorological Center/National Weather Service, Washington, D.C. 20233. John M. Wallace is a professor in the Department of Atmospheric Sciences and director of the Joint Institute for the Study of the Atmosphere and Ocean, University of Washington, Seattle 98195.

from season to season. The host of studies in the years since Bjerknes's work provide a much more complete description of the ENSO phenomenon, which emerges as the dominant global climate signal on time scales of a few months to a few years (7-10).

Some of the relations identified and documented in these studies are implicit in the time series in Fig. 1. The vertical lines correspond to ENSO episodes as defined by equatorial SST, rainfall at island stations in the equatorial central Pacific, and sea-level pressure at Darwin, Australia (Fig. 1, A to C). Note the almost perfect correspondence among these three series, whose mutual correlation coefficients all exceed 0.8. The spacing of the individual episodes ranges from 2 years to about a decade. In a few cases, such as 1976 to 1978, a single episode spans several consecutive years. The negative correlation between series C and D in Fig. 1 illustrates the east-west seesaw in sea-level pressure noted by Walker and earlier investigators (11). Selected relations involving rainfall in other parts of the tropics and subtropics are indicated by series E, F, and G, and

relations involving regional climate anomalies at extratropical latitudes are illustrated by the remaining time series. The climate variables indicated by asterisks were considered by Walker to be involved in the Southern Oscillation; hence the segments of those time series from the late 1920's on may be regarded as confirmation of his findings.

The time series in Fig. 1 do not resolve the spatial structure and time history of individual ENSO episodes and their strong seasonal dependence. We will return to that subject presently, but first we will describe a conceptual framework for interpreting some of the atmospheric phenomena associated with these episodes.

A Conceptual Framework

A meteorologist may think of the Southern Oscillation as the atmospheric response to a prescribed SST anomaly, just as an oceanographer may treat El Niño as a response to a prescribed wind stress at the sea surface. Both approaches are limited but nevertheless valid in

the sense that they lead to well-posed, relatively tractable scientific questions whose answers are prerequisites for effectively addressing the much more difficult problem of coupled atmosphere-ocean interactions in the time-dependent climate system. Throughout this section we will adopt the parochial perspective of the meteorologist.

The mechanisms through which SST anomalies in the equatorial Pacific might produce the worldwide climate anomalies described in Fig. 1 have been a subject of intense debate in the recent meteorological literature. Although many aspects of the workings of the global climate system have yet to be resolved, the broad outlines of a theory explaining the linkages between equatorial SST, tropical precipitation, global circulation patterns at the jet stream level (10 km), and climate anomalies at the earth's surface are beginning to emerge.

On time scales of weeks and longer and on space scales of more than 1000 km, the primary way in which the tropical atmosphere responds to temperature contrasts at the earth's surface is through thermally direct circulations. In such circulations the warmest regions at the earth's surface are characterized by ascent of moisture-laden air from the planetary boundary layer that condenses to form widespread cloudiness and precipitation. Elsewhere there is subsidence of dry air from the upper troposphere, forming a lid on the planetary boundary layer and preventing small trade-wind cumulus clouds from growing to a size that can produce substantial rainfall. Examples of such thermally direct circulations are the monsoons, which bring heavy rainfall to the subtropical continents during summertime, when they are warmer than the surrounding ocean.

Over the equatorial Pacific there is usually a strong SST gradient, with relatively cool waters in the east and warmer (by 3 to 6 K) waters in the west toward New Guinea. This east-west gradient is associated with a thermally direct circulation in the equatorial plane, with (i) sinking motion in the eastern Pacific, (ii) westward low-level flow (the equatorial extension of the trade winds), (iii) rising motion and deep cumulus convection over the extreme western Pacific and Indonesia, and (iv) eastward return flow at the cirrus cloud level (10 to 15 km). Bjerknes (12) referred to this circulation cell as the Walker circulation in memory of Sir Gilbert Walker. Under normal conditions, rainfall at equatorial stations near or east of the date line is virtually nil because of the large-scale subsidence associated with the Walker circulation.

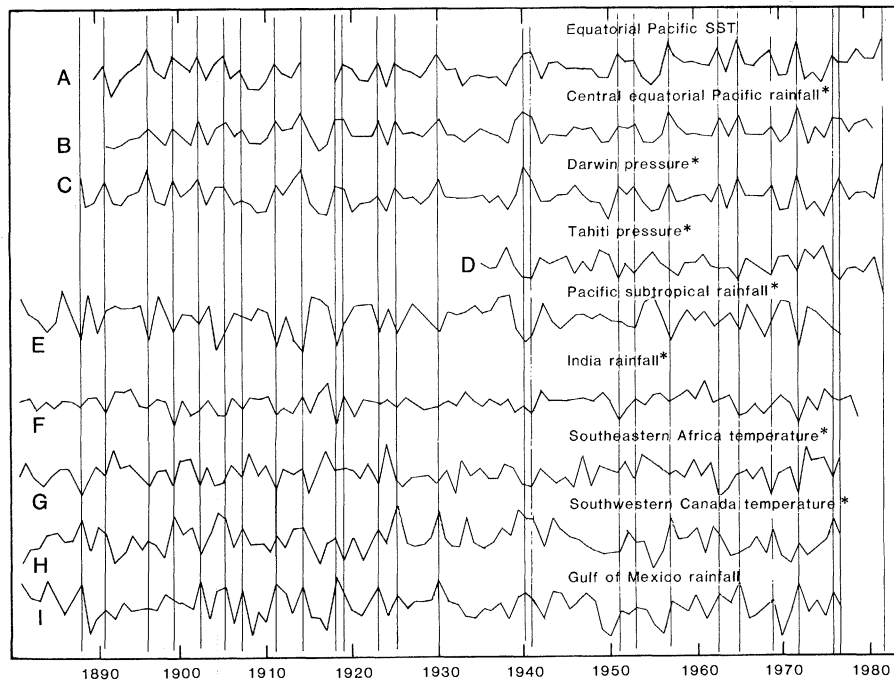


Fig. 1. Time series of selected variables whose interannual variability is related to the ENSO phenomenon. Each data point represents an average over 1 year or a season, as indicated, where the years on the horizontal axis refer to the beginning of the averaging periods. (A) Equatorial eastern Pacific (South American coast to the date line) SST, April to March; (B) rainfall index for central equatorial Pacific island stations, April to March; (C) sea-level pressure at Darwin, Australia (12°S, 131°E), April to March; (D) sea-level pressure at Tahiti (17°S, 150°W), April to March; (E) rainfall index for the subtropical North Pacific, November to May; (F) rainfall index for India, June to September; (G) rainfall index for southeastern Africa, November to May; (H) temperature index for stations in southwestern Canada and the northwestern United States, November to April; and (I) rainfall index for stations in northern Mexico and the U.S. Gulf Coast, November to February. Vertical lines indicate ENSO episodes as inferred from the top three series. Further details and quantitative values are available from E.M.R.

During ENSO episodes the equatorial waters in the eastern half of the Pacific are warmer than normal while SST's west of the date line are near or slightly below normal, so that the east-west temperature gradient is diminished and waters near the date line may be as warm as those anywhere to the west ($\sim 29^{\circ}\text{C}$). The region of heavy rainfall shifts eastward so that Indonesia and adjacent regions experience drought while the desert islands in the equatorial central Pacific experience month after month of torrential rainfall. Near and to the west of the date line the usual easterly surface winds along the equator weaken or shift to westerly (which has implications for the ocean dynamics), while anomalously strong easterlies are observed at the cirrus cloud level.

The effects of the equatorial SST anomalies would be confined to the equatorial belt were it not for the earth's rotation, which makes it possible for changes in the tropical circulation to excite a large-scale quasi-stationary wave pattern, best defined in the upper troposphere, that can give rise to substantial anomalies in the extratropical circulation. The pattern of upper tropospheric circulation anomalies associated with ENSO episodes during the Northern Hemisphere winter is illustrated in Fig. 2A, which is based on a composite of past events (8). Note the anticyclonic circulation anomalies straddling the region of enhanced rainfall in the equatorial Pacific, with one center near Hawaii and the other near 20°S . These anticyclonic gyres can be understood as a direct response to the upper-level divergence from the region of heavy rainfall, which, in the presence of the earth's rotation, leads to the production of anticyclonic vorticity along its poleward flanks. Poleward and eastward of the center near Hawaii in Fig. 2A is an apparent wave train with a negative center over the North Pacific, a positive center over western Canada, and another negative center over the southeastern United States. The "centers of action" associated with this wave train lie along a broad "great circle" arc. The dispersion of these so-called Rossby waves is now widely believed to be the dynamic mechanism responsible for the strong temporal correlations between tropical and extratropical climate anomalies such as those shown in Fig. 1. Although Walker postulated the existence of such a mechanism long ago, the basic theoretical concepts did not appear in the meteorological literature until the late 1970's (13), and it was not until the early 1980's that their relevance to the ENSO

problem was fully recognized (8, 14).

The dynamics of Rossby wave trains emanating from regions of enhanced tropical rainfall have been intensively investigated during the past few years with a variety of simple dynamic models. Among the insights derived are the following:

1) The magnitude of the extratropical response appears to be sensitive to the background flow on which the equatorial rainfall anomaly is superimposed. In particular, the extratropical response in the models is enhanced by the presence of the climatological mean stationary wave pattern forced by the major mountain ranges and land-sea heating contrasts (15).

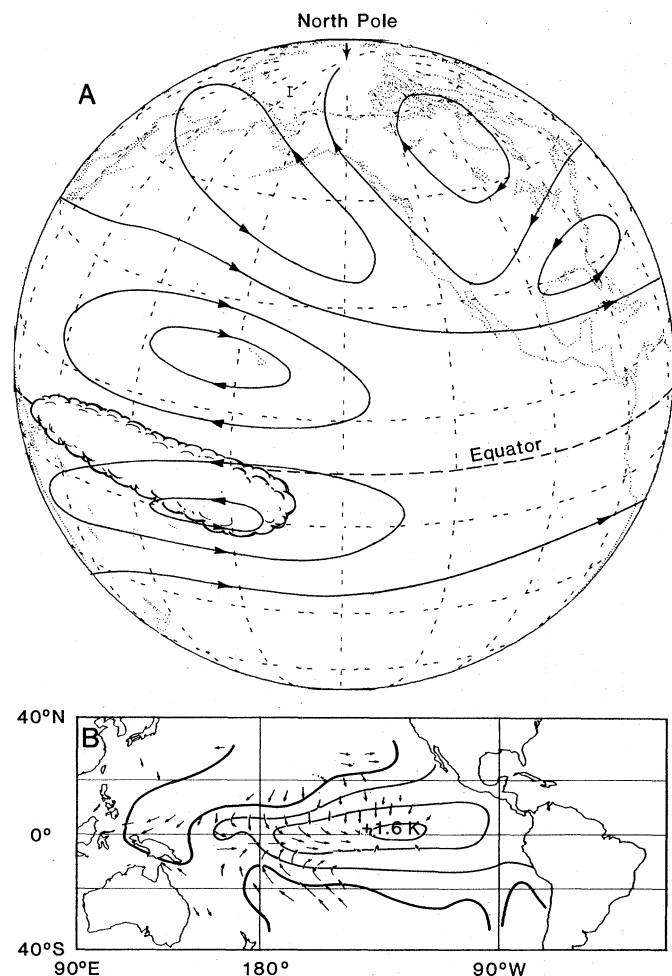
2) In the Northern Hemisphere during wintertime, when the stationary waves are very strong, the response in the models takes the form of a geographically fixed normal mode, which resembles the pattern in Fig. 2. That is, when the region of enhanced rainfall is moved eastward or westward along the equator, the shape and geographical location of the simulated extratropical response remains as in Fig. 2, although the amplitude and perhaps even the polarity

change. This normal-mode behavior is associated with barotropic instability of the climatological mean flow pattern and may be excited in many different ways: forcing by equatorial rainfall anomalies is just one possibility (16).

3) Nonlinear interactions between the background flow and the circulation anomalies forced by the perturbations in equatorial rainfall may be important, particularly in the tropics. Hence the atmospheric response at a given time may depend on the time history of the atmospheric circulation during previous months (17).

It is possible to model the atmospheric response to a prescribed SST anomaly without referring to any of the dynamic concepts mentioned above, but using instead state-of-the-art general circulation models (GCM's) (18), which are capable of realistic simulations of global climate, including the normal annual cycle. A number of GCM experiments have been conducted over the past 10 years at various institutions. Most of these experiments consist of a pair of simulations, one with a prescribed SST distribution based on climatological mean conditions and the other with a distribu-

Fig. 2. Schematic illustration of atmospheric conditions during winter in the Northern Hemisphere after the peak of a typical ENSO episode, based on the understanding of the phenomenon before the 1982-1983 episode. (A) Region of enhanced precipitation (cloud outline) and circulation anomalies at the jet stream ($\sim 10\text{-km}$) level. (B) SST and surface wind anomalies (contour interval, 0.5 K ; zero contour is heavier). The longest arrows correspond to wind anomalies of $\sim 1.5\text{ m/sec}$ (8, 9).



tion based on typical conditions during ENSO episodes. The results of these experiments show a remarkably consistent pattern that is in general agreement with observations. The models correctly simulate the observed eastward shift of the region of heavy rainfall from the extreme western Pacific toward the central Pacific, the upper level anticyclone pair straddling the region of enhanced precipitation, and most of the experiments based on wintertime conditions in

the Northern Hemisphere show evidence of teleconnections to extratropical latitudes that are reminiscent of the pattern in Fig. 2 (19), and consistent with the relations in Fig. 1, H and I. The one experiment that has been conducted for summertime conditions showed evidence of a suppression of the Indian monsoon rainfall, in agreement with Fig. 1 (20).

Both GCM's and much simpler models are capable of simulating the diminished

easterly flow along the equator near and just west of the region of enhanced rainfall (Fig. 2B) and the related changes in sea-level pressure (Fig. 1, C and D) observed during episodes of warm SST's in the equatorial Pacific. It is these same changes in surface wind over the tropical Pacific that physical oceanographers use in modeling the time variability of equatorial SST's. Hence it appears that the atmospheric models contain many of the basic ingredients required to simulate the atmosphere-ocean system. However, thus far the atmospheric modeling experiments have not addressed the time-dependent aspects of the ENSO problem in a way that takes into account the large observed mean annual cycle in SST's in the eastern equatorial Pacific and the evolution of SST anomalies relative to that seasonally varying climatological mean.

The 1982-1983 ENSO episode provided scientists with an opportunity to test this conceptual framework on the basis of a new, independent set of data.

Delayed Onset of the 1982-1983 Episode

Scientists were caught off guard by the unusual timing of the onset of the 1982-1983 episode relative to the climatological mean annual cycle. A composite description, based on the six major events that occurred between 1950 and 1975 (9), is dominated by the positive SST anomalies, approaching 2 K, appearing first along the South American coast early in the calendar year and spreading westward to cover the entire equatorial region east of 170°E by July. Most of these events were preceded by a period of abnormally strong easterly surface winds along the equator to west of the date line. The winds weakened abruptly around November, coincident with a swing in the Southern Oscillation associated with the partial collapse of the surface anticyclone in the southeast subtropical Pacific. The resulting change in surface wind stress along the equator was believed to be responsible for the onset of warm SST's (21). These precursors in the surface wind and sea-level pressure fields were not observed during 1981 or early 1982. Furthermore, it is evident from Fig. 3B that there was no dramatic warming of surface waters along the South American coast during early 1982; SST at Puerto Chicama on the coast of Peru did not begin to rise sharply until September and October 1982. Similar timing with respect to the climatological mean annual cycle was observed in the

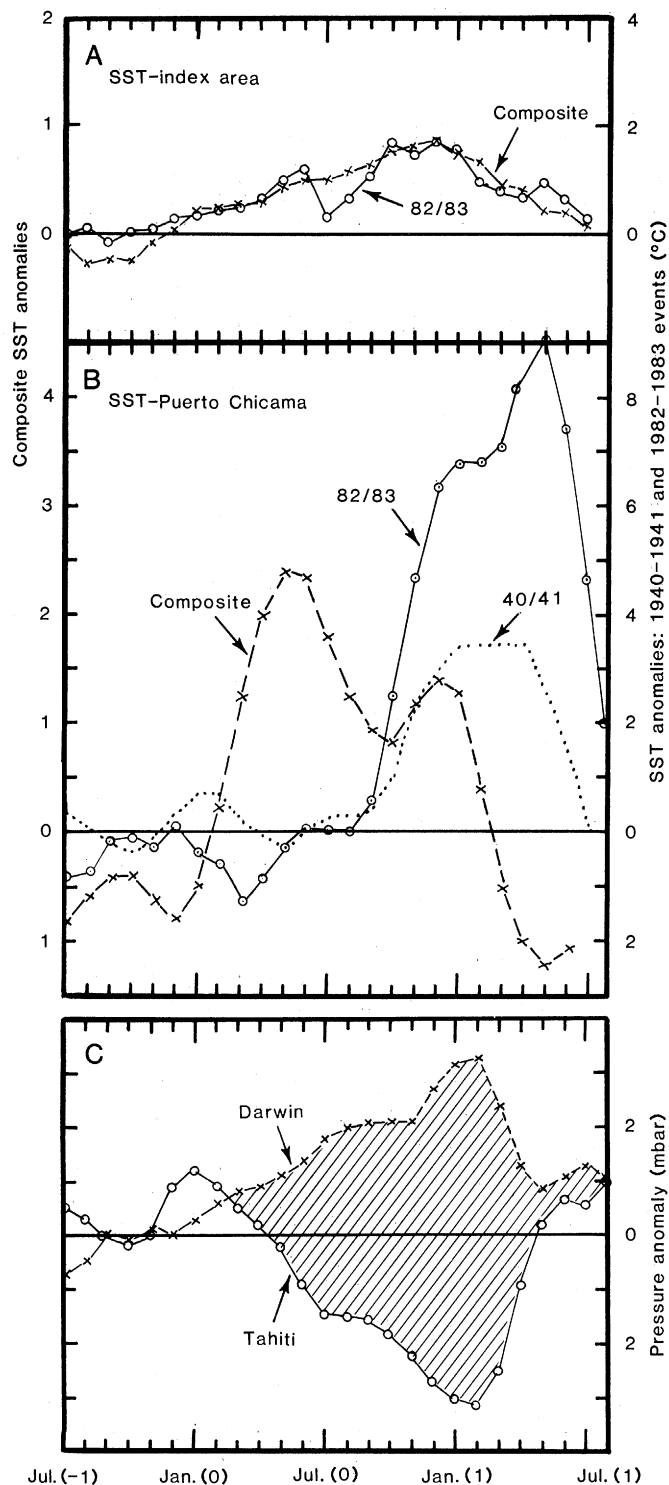


Fig. 3. (A) Monthly running mean SST anomalies for the region from 4°N to 4°S and 150°W to 160°E. (B) Three-month running mean SST anomalies for Puerto Chicama (7.7°S, 79.3°W). Continuous and dotted lines refer to the 1982-1983 and 1940-1941 episodes, respectively. For these two curves, year 0 on the abscissa refers to 1982 and 1941, respectively. The dashed curve refers to a composite of six warm episodes between 1950 and 1975 (9). The ordinate scales for the 1982-1983 and 1940-1941 events (right) represent SST anomalies twice as large as those represented by the corresponding scale (left) for the composite event. (C) Sea-level pressure anomalies at Tahiti (17°S, 150°W) and Darwin (12°S, 131°E) during the 1982-1983 episode. The difference between the two pressures (Tahiti minus Darwin), indicated by shading, is often used as an index of the Southern Oscillation.

1940–1941 event, which, by some measures at least, was the strongest event on record before the recent one (22).

Farther to the west, the contrast between the timing of the composite ENSO warming and the 1982–1983 episode is much less striking. In most of the six events in the composite, small but possibly significant increases in SST were observed along the equator in the vicinity of the date line as early as December or January. In the 1982–1983 episode, mean equatorial SST between 150°W and 160°E (Fig. 3A) began rising at the usual time and, apart from the curious dip during July, followed a course very similar to that in the composite.

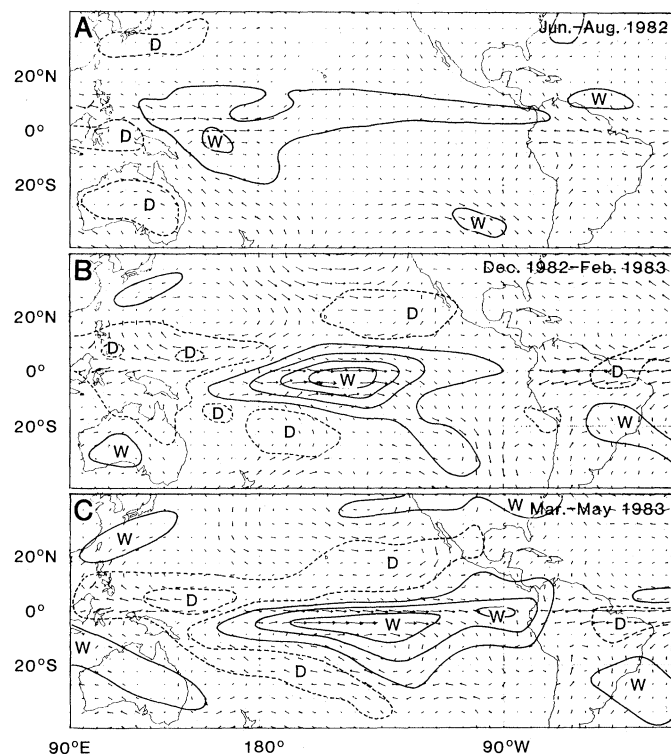
Although the initial anomalies were generally less than 1 K, they were large enough to shift the location of the warmest surface waters eastward by as much as 30°. Whether these subtle changes in SST in the central Pacific were instrumental in setting the stage for the more dramatic atmospheric changes that took place a few months later is unknown.

The results shown in Fig. 3 deserve comment in relation to the widely publicized suggestion that the eruption of El Chichón played an essential role in triggering the 1982–1983 ENSO episode (23). The evidence put forth in support of this suggestion—that the recent episode was unprecedented in its strength and timing relative to the annual cycle and that its onset followed the volcanic eruption closely—is largely circumstantial. In our view, the apparent similarities between the 1940 and 1982 episodes with respect to intensity and timing, together with the evidence of a rising trend in SST anomalies over much of the equatorial Pacific before the eruption, cast doubt on these arguments.

A Swing in the Southern Oscillation

In the composite ENSO episode the decline in sea-level pressure (relative to the climatological mean annual cycle) that begins in the southeast subtropical Pacific around November continues through the following August, while pressure in the broad region that forms the western end of the seesaw rises. Meteorologists refer to these pressure changes as a swing of the Southern Oscillation. In the composite event the sea-level pressure difference, Darwin minus Tahiti, which is often used as an index of the oscillation, drops from about 1 mbar above normal in November at the onset of the event, to near normal in January, to almost 2 mbar below normal in Au-

Fig. 4 (A to C) Anomalies in satellite-sensed outgoing longwave radiation (OLR) (contours) and wind at 850 mbar (arrows) for three seasons during the 1982–1983 episode. Negative anomalies in OLR, indicated by the solid contours and labeled W for “wet,” correspond to regions of enhanced precipitation, and vice versa (D, “dry”). Contour interval, 20 W/m² (where contours correspond to ±10, ±30, and so forth). The longest arrows correspond to wind anomalies on the order of 10 m/sec.



gust. Toward the end of this period there is usually a more pronounced weakening or even a reversal of the surface easterlies along the equator in the vicinity of the date line, accompanied by a further eastward shift of the rain area from the western Pacific to near the date line.

The 1982–1983 episode was characterized by an unusually abrupt swing of the Southern Oscillation, which began late but quickly overtook its counterpart in the composite. Between April and August 1982 the sea-level pressure difference between Tahiti and Darwin dropped from near normal to about 3 mbar below normal (Fig. 3C). In June the easterly surface winds along the equator to the west of the date line shifted abruptly to fitful westerlies (24). This wind shift marked the onset of an extended period of extremely heavy precipitation in the equatorial central Pacific. Farther to the west, Indonesia, eastern Australia, Melanesia, Southern India, Sri Lanka, and southern Africa were experiencing the beginning of a severe, and in some places record, drought, with attendant crop losses and the threat of famine (25, 26).

Anomalies in wind and precipitation for the period June to August 1982 are illustrated in Fig. 4A. The arrows represent wind anomalies at the 850-mbar (~1.5-km) level and the contours represent anomalies in outgoing infrared radiation sensed from satellites. Regions of enhanced mid-altitude and high clouds,

which normally accompany convective precipitation in the tropics, show up as negative anomalies because clouds in the cold middle and upper troposphere emit less radiation to space than the warmer earth's surface. Note the strong correspondence between the regions of enhanced precipitation, convergence, and westerly wind anomalies in the equatorial belt.

A Sharp Rise in SST

September and October 1982 were marked by dramatic rises in SST and sea level along the South American coast and throughout the eastern equatorial Pacific. These changes followed, by about 3 months, the abrupt shift in low-level winds west of the date line from easterly to westerly and the corresponding east-west seesaw in sea-level pressure. A similar phase lag is observed in the composite ENSO episode, in which the events in question begin 6 months earlier. Hence the new observations support the idea that the rising SST in the eastern Pacific is a response to abrupt changes in surface wind stress west of the date line.

Coincident with the rises in SST in the eastern Pacific, the intertropical convergence zone, a narrow east-west band of heavy precipitation that, at this time of year, normally lies near 10°N, shifted southward toward the equator, and a

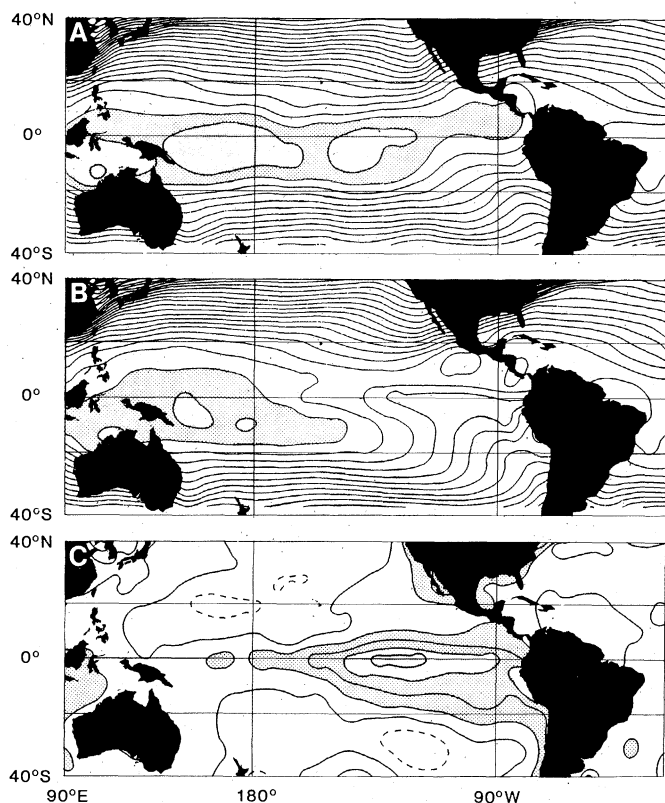


Fig. 5. Sea-surface temperature patterns (contour interval, 1 K). (A) December 1982 to February 1983. (B) December-February climatology. The heaviest shading corresponds to SST's $> 29^{\circ}\text{C}$. (C) Anomalies for December 1982 to February 1983. The heaviest shading denotes anomalies > 3 K.

prolonged period of heavy precipitation began in Ecuador and northwestern Peru, several months in advance of the normal wet season. Rainfall records were shattered month after month from November through June. For example, Guayaquil, Ecuador, recorded a total of 2636 mm in the 6-month interval from November to April, compared with the previous record of 1670 mm set during the 1972-1973 ENSO episode (27). Ironically, while the desert regions of northwest Peru received record rainfall, major agricultural areas in southern Peru and northern and central Bolivia were experiencing serious drought (28).

Peak of the 1982-1983 Episode

December 1982 to February 1983 saw further intensification and extension of the anomaly patterns of the previous months. Drought in southern Africa, southern India and Sri Lanka, and the Australian-Indonesian region continued and, as in past ENSO episodes, expanded to cover the boreal subtropical Pacific from the Philippines eastward through the Hawaiian Islands. The deluge continued over Ecuador and northern Peru.

Figure 5 shows the observed SST pattern for December 1982 to February 1983, the climatological mean pattern for that season, and the corresponding SST anomaly pattern, which is simply the

difference between the two fields. The SST anomaly pattern resembles the composite pattern based on previous ENSO episodes for December to February (approximately 1 year after the onset of warm SST's along the South American coast), except that the magnitude of the warm anomalies is more than twice as large as in the composite pattern (9). The anomalies for 1982 to 1983 were so large that it was nearly as warm along the South American coast as in the western Pacific, and the warmest SST's in the equatorial belt crossed the date line and extended considerably farther to the east than in the composite of past episodes. The Southern Oscillation index (sea level pressure at Tahiti minus that at Darwin) took another sharp downward swing from 4 mbar below normal in November 1982 to an unprecedented 6 mbar below normal in February 1983 (Fig. 3C).

The anomaly charts for wind at 850 mbar and outgoing infrared radiation for December 1982 to February 1983 are shown in Fig. 4B. The drought areas mentioned above show up as positive anomalies in outgoing infrared radiation. As in Fig. 4A, there is a strong correspondence between the region of enhanced cloudiness and precipitation (negative anomalies in outgoing infrared radiation) and the region of westerly wind anomalies along the equator. Compared to the June-August pattern shown in Fig. 4A, the region of enhanced pre-

cipitation lies farther to the east. This gradual eastward shift of the rain area, surface westerly wind anomalies, and maximum SST is a striking characteristic of the time history of the 1982-1983 episode. A comparison of Figs. 2 and 4 shows that at this season the rain area along and south of the equator was shifted farther east than in the composite. With it, the region of tropical storm genesis in the South Pacific shifted far to the east and, as a result, French Polynesia, noted for its benign climate, was battered by five full-blown hurricanes (29, 30).

Figure 6 shows the circulation anomalies at the jet stream level (200 mbar) during December 1982 to February 1983. As in Fig. 2, the pattern is characterized by anticyclonic gyres straddling the equator, with easterly wind anomalies covering the region of enhanced rainfall over the equatorial central Pacific and westerly wind anomalies at subtropical latitudes of both hemispheres. Cyclonic circulation anomalies covered the North Pacific from the ocean surface to the tropopause. In this region, mean sea-level pressures and upper level geopotential heights exhibited record low values and numerous storms exhibited central pressures below 950 mbar (31). This observation is in agreement with Fig. 2 and with the results of GCM simulations.

The anticyclonic circulation anomaly over south-central Canada is slightly farther east than its counterpart in Fig. 2. This feature and the southerly flow along its western flank was associated with a belt of unusually mild wintertime temperatures (up to 6 K above normal) centered along the border between the United States and Canada from Lake Superior westward to the Pacific. This region of above-normal temperatures corresponds closely to that observed during past ENSO episodes (Fig. 1H).

The most striking climate anomalies observed over the United States during this period were those associated with westerly wind anomalies extending across the subtropical Pacific, the southern border of the United States, and the Gulf of Mexico (Fig. 6). Such wind anomalies indicate a pronounced intensification and southward displacement of the normal westerly jet stream that sweeps across this region. Associated with this intensified jet stream were an unusual number of winter storms that battered the California coast with high winds, brought flooding to parts of California and the Gulf states, and buried mountain regions of the Southwest with heavy snow in late winter and spring (32). Abnormally wet winters in the Gulf

states have been observed in association with past ENSO episodes (Fig. 1I) and in some of the GCM simulations.

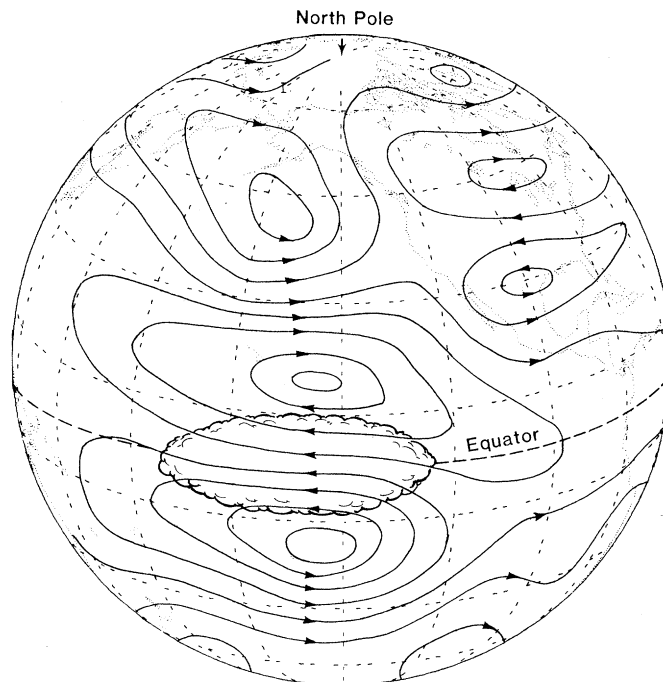
Not all of the major climate anomalies of the 1982–1983 winter can be unambiguously interpreted as interlocking pieces of the ENSO jigsaw puzzle. Wet, stormy winters over California and other parts of the Southwest have occurred during warm episodes in the equatorial Pacific (such as 1977–1978), but there have also been abnormally dry winters during warm episodes (such as 1976–1977). So when the entire historical record is taken into account the correlations between various indices of the ENSO phenomenon and California rainfall are not very impressive. Despite some dramatic examples of cold winters over the eastern United States during past ENSO episodes (for example, 1957–1958, 1969–1970, 1976–1977, and 1977–1978), the correlations involving winter temperatures for this region as a whole are not very strong either, and the 1982–1983 episode turned out to be somewhat warmer than normal throughout most of the region. One of the most remarkable anomalies of the winter of 1982–1983 was the abnormal warmth across not only North America but also most of Eurasia at latitudes near 50°N (31). There is no evidence of a systematic pattern of anomalies over Eurasia during ENSO episodes. Likewise, over the Atlantic sector there were large anomalies in the pressure and wind fields. Note, for example, the easterly wind anomalies over Brazil (Fig. 4, A to C) (3, 33). These unexplained anomalies serve as a reminder that only a part of the year-to-year climate variability can be regarded as part of the ENSO signal, even in years when that signal is very strong.

Return to Normal Conditions

Many aspects of the pattern described in the previous section persisted through March, April, and May 1983. The anomalous wind pattern and equatorial rainfall continued but weakened through May (Fig. 4C). Pressure remained well below normal in the North Pacific, and the storm track across the southern United States remained active through much of April.

The decay phase, like the onset phase, appeared to be preceded by a dramatic swing in the Southern Oscillation back to near-normal conditions from February to May 1983 (Fig. 3C). While the atmospheric circulation was returning to normal, SST along the South American coast remained nearly constant, then be-

Fig. 6. Atmospheric conditions for December 1982 to February 1983 (compare Fig. 2A).



gan to fall. But the decrease was less than the normal seasonal change, so there was actually a second increase in the SST anomalies. Peak anomaly values, in excess of 8 K near South America, were reached in May and June. This second maximum was largely confined to the eastern equatorial Pacific. Farther west, anomalies continued to decrease slowly from their peak in November and December (Fig. 3, A and B). The second rise near South America might have been a response to the second sharp downward swing of the Southern Oscillation index that took place 3 to 4 months earlier (Fig. 3C).

Sea-surface temperature anomalies near the South American coast underwent an abrupt decrease during early July, followed by a more gradual decrease through September 1983. These changes may have been a response to the swing of the Southern Oscillation back toward normal from February to May. Although the normal low-level wind pattern has been reestablished along the equator at this writing, SST east of 140°W is still well above normal, and the associated area of heavy rainfall, which migrated northward from Ecuador and northwest Peru during June and July, is still in evidence north of the equator.

Discussion

The peculiar time history of the 1982–1983 ENSO episode invites speculation as to whether all such episodes might be viewed as a superposition of two, inter-

related kinds of events, which have much in common and usually occur in combination about 6 months apart:

1) An enhancement of the mean annual cycle in SST, largely confined to the eastern third of the Pacific, with maximum amplitude near the South American coast. Positive SST anomalies developing rather abruptly along the coast during January or February and spreading westward, peaking in May or June, and disappearing by September or October. A response to the swing of the Southern Oscillation, associated with the sudden weakening of the southeast Pacific anticyclone near Tahiti starting around November of the previous year.

2) A broader scale warming of the equatorial Pacific from near the date line eastward, with maximum amplitude from 90° to 150°W, starting around the middle of the calendar year, peaking near the end of the year, and disappearing a few months later. A response to a swing in the Southern Oscillation involving sea-level pressure rises at the western end of the seesaw (near Darwin).

Events of the first kind conform to oceanographers' notion of El Niño in its purest form, while events of the second kind are more important from a meteorological perspective because of their much broader longitudinal extent. One might think of a typical ENSO episode, as exemplified by the composite (9), as consisting of an event of the first kind followed, with some overlap, by an event of the second kind. The 1982–1983 episode can be interpreted in terms of the reverse sequence, commencing in

1982 with an unusually intense broad-scale warming and followed, in the first half of 1983, by a more localized warming of the first kind that is at this writing in its decaying phase.

Whether this interpretation is valid or useful remains to be seen. In any case, the 1982–1983 episode brings into sharper focus a series of probing “chicken and egg” type questions concerning the nature of atmosphere-ocean interactions in the tropics.

1) What are the processes responsible for the pronounced and unexpected swings of the Southern Oscillation during this and other ENSO episodes? Is the atmosphere somehow responding, in an exaggerated way, to subtle changes in the tropical Pacific SST pattern, or is it switching between different circulation regimes for other reasons?

2) Why did the heaviest rainfall, the surface westerlies, and the warmest SST's gradually migrate eastward across the equatorial Pacific during the episode?

3) What is the role of the annual cycle in the initiation, evolution, and decay of this and other episodes?

The recent episode also raises questions about the relation between the ENSO phenomenon and climate anomalies throughout the world:

1) Were the unusually strong westerly flow and storminess over the the south-western United States and the unusual warmth over Eurasia related to the ENSO episode or did they occur for other reasons?

2) Is it possible to distinguish between episodes like the most recent one, characterized by mild conditions over much of the northern United States, and those such as the 1976–1977 episode, in which the East was significantly colder than normal?

Such questions will be the focus of an extensive national research program on the ENSO phenomenon, now in the planning stage.

References and Notes

1. G. T. Walker, *Mem. Indian Meteorol. Dep.* **24**, 275 (1924).
2. — and E. W. Bliss, *Mem. R. Meteorol. Soc.* **4**, 53 (1932).
3. H. P. Berlage, *K. Ned. Meteorol. Verh.* **88** (1966), entire volume.
4. R. B. Montgomery, *Mon. Weather Rev.* **39** (Suppl.), 1 (1940).
5. J. Namias and D. R. Cayan, *Science* **214**, 869 (1981); T. Ichiye and J. Petersen, *J. Meteorol. Soc. Jpn.* **41**, 172 (1963); R. Doberitz, *Bonn. Meteorol. Abh.* **8**, 1 (1968).
6. J. Bjerknes, *Tellus* **18**, 820 (1966); *Mon. Weather Rev.* **97**, 163 (1969); *J. Phys. Oceanogr.* **2**, 212 (1972).
7. K. E. Trenberth, *Q. J. R. Meteorol. Soc.* **102**, 639 (1976); B. C. Weare, A. R. Navato, R. E. Newell, *J. Phys. Oceanogr.* **6**, 671 (1976); T. P. Barnett, *ibid.* **7**, 633 (1977); E. R. Reiter, *Mon. Weather Rev.* **106**, 324 (1978); W. H. Quinn, D. O. Zopf, K. S. Short, R. T. W. K. Yang, *Fish. Res. Bull.* **76**, 663 (1978); P. R. Julian and R. M. Chervin, *Mon. Weather Rev.* **106**, 813 (1978); C. S. Ramage and A. M. Hori, *ibid.* **109**, 1827 (1981); P. A. Arkin, *ibid.* **110**, 1393 (1982); Y. H. Pan and A. H. Oort, *ibid.* **111**, 1244 (1983); S. G. H. Philander, *Nature (London)* **302**, 295 (1983).
8. J. D. Horel and J. M. Wallace, *Mon. Weather Rev.* **109**, 813 (1981).
9. E. M. Rasmusson and T. H. Carpenter, *ibid.* **110**, 354 (1982).
10. H. van Loon and R. A. Madden, *ibid.* **109**, 1150 (1981).
11. H. H. Hildebrandsson, *K. Svenska Vetensk.-Akad. Handl.* **29**, 1 (1897); N. Lockyer and W. J. S. Lockyer, *Proc. R. Soc. London Ser. A* **73**, 457 (1904).
12. J. Bjerknes, *Mon. Weather Rev.* **97**, 163 (1969).
13. B. J. Hoskins, A. J. Simmons, D. G. Andrews, *Q. J. R. Meteorol. Soc.* **103**, 553 (1977).
14. A. E. Gill, *ibid.* **106**, 447 (1980); B. J. Hoskins and D. J. Karoly, *ibid.* **107**, 1179 (1981); J. D. Opsteegh and H. M. Van den Dool, *J. Atmos. Sci.* **37**, 2169 (1980); P. J. Webster, *ibid.* **38**, 554 (1981); *ibid.* **39**, 41 (1982).
15. A. J. Simmons, *Q. J. R. Meteorol. Soc.* **108**, 502 (1982); P. J. Webster and J. R. Holton, *J. Atmos. Sci.* **39**, 722 (1982); G. W. Branstator, *ibid.* **40**, 1689 (1983).
16. A. J. Simmons, J. M. Wallace, G. W. Branstator, *J. Atmos. Sci.* **40**, 1363 (1983).
17. K.-M. Lau and H. Lim, *ibid.*, in press.
18. These numerical models are based on the governing equations for large-scale atmospheric motions in a global domain, and are similar to those used in weather forecasting but integrated for 1 month of simulated time or longer to generate climate statistics.
19. P. R. Rountree, *Q. J. R. Meteorol. Soc.* **98**, 290 (1972); J. Shukla and J. M. Wallace, *J. Atmos. Sci.* **40**, 1613 (1983); M. L. Blackmon, J. E. Geisler, E. J. Pitcher, *ibid.*, p. 1410.
20. R. N. Keshavamurty, *J. Atmos. Sci.* **39**, 1241 (1982).
21. K. Wyrski, *J. Phys. Oceanogr.* **5**, 572 (1975); A. J. Busalacchi and J. J. O'Brien, *J. Geophys. Res.* **86**, 10,901 (1981).
22. Little is known about SST patterns farther to the west over the open ocean during 1940 to 1941 because the retrieval of merchant ship observations was disrupted during World War II.
23. R. A. Kerr, *Science* **219**, 157 (1983).
24. In a letter to J. Rasmusson (director, NOAA Climate Analysis Center) dated 17 January 1983, B. Onorio (chief fisheries officer, Tarawa, Republic of Kiribati) noted, “Our area has been getting constant waves and westerly winds disrupting fisheries operations. More recently winds have been unusually strong easterly.” (The return to strong easterly flow occurred late in 1982.)
25. E. M. Rasmusson and J. M. Hall, *Weatherwise* **36**, 164 (1983).
26. Washington Post, 4 February 1983; J. L. Rowe, Jr., and T. B. Edsall, *ibid.*, 18 February 1983, p. A1; R. Hoyle, *Time* (Asian edition), 28 March 1983, p. 6; M. von Dijk, D. Mercer, J. Peterson, *New Sci.*, 7 April 1983, p. 30; *U.S. News World Rep.*, 11 April 1983, p. 48; J. Kapstein, *Bus. Week*, 25 April 1983, p. 6; J. Lelyveld, *New York Times*, 18 May 1983, p. 6.
27. Special El Niño report prepared by the Ecuadorian Naval Oceanographic Institute, Guayaquil, Ecuador (April 1983).
28. P. Bennett, Washington Post, 28 May 1983, p. A2; P. J. Hilts, *ibid.*, 11 June 1983, p. A1; J. Diehl, *ibid.*, 31 July 1983, p. A17; M. deC. Hinds, *New York Times*, 2 June 1983, p. A8; E. Schumacher, *ibid.*, 12 June 1983, p. A1.
29. D. DeAngelis, *Mar. Weather Log* **27**, 106 (1983).
30. In a letter to J. Rasmusson dated 15 February 1983, J. Couchard (chief, FAAA Meteorological Center, Tahiti) noted, “We experienced a tropical hurricane in January and have to go back to 1906 for recording so strong a tropical cyclone in the Tuamotu archipelago. Marquesas Islands reported rain quantities as never recorded before. From November, 1982, the total is about five times in excess of the mean value.” Subsequently the Marquesas station at Atuona recorded 2952 mm of rainfall from January through April (compared to a mean of 398 mm), and the most devastating hurricane of modern times struck Tahiti in April 1983. In the Northern Hemisphere an unusual hurricane (Iwa), moving northward from the region of warm water, caused extensive damage in the Hawaiian Islands in late November 1982, almost 25 years to the day since a similar storm struck the islands during the warm episode of 1957 [H. E. Rosendal, *Mar. Weather Log* **27**, 63 (1983)].
31. R. S. Quiroz, *Mon. Weather Rev.*, in press.
32. A. Gullenhaal, *Miami Herald*, 19 February 1983, p. 1; B. Siegel, *Los Angeles Times*, 17 August 1983, p. 1.
33. Outgoing longwave radiation data show below-normal rainfall over parts of northeastern South America during late 1982 and early 1983 (Fig. 4). Such anomalies are common at this stage of a warm episode [G. T. Walker, *Q. J. R. Meteorol. Soc.* **54**, 79 (1982); C. N. Cavides, *Proc. Assoc. Am. Geogr.* **5**, 44 (1973)]. On the other side of the Atlantic, D. C. Duffy (Beneguela Ecology Programme, University of Cape Town), in a letter to the NOAA Climate Analysis Center dated 15 March 1983, reported reduced upwelling in the southern African area during the 1982–1983 event. L. V. Shannon (unpublished manuscript, Sea Fisheries Research Institute, Cape Town, South Africa) stated, “Inspection of our past records of warm and El Niño type events shows that similar perturbations [reduced upwelling along the Cape west coast] were evident.” The eastern North Atlantic–western European sector has not shown a consistent ENSO anomaly pattern (10).
34. We thank P. A. Arkin and R. W. Reynolds for preparing the analysis products for the 1982 event and P. B. Wright and T. H. Carpenter for constructing the historical indices. Recent SST data for Puerto Chicama were provided by D. V. Hansen. The work of J.M.W. was supported by NSF grant 81-06099.